

Crystal structure and Hirshfeld surface analysis of *N*-(4-nitrophenyl)-2-(piperidin-1-yl)acetamide (lidocaine analogue)

Imane Maimoune,^{a,b} Benson M. Kariuki,^c Abderrazzak El Moutaouakil Ala Allah,^b Intissar Nchioua,^b Abdulsalam Alsubari,^{d*} Joel T. Magee,^e Abdelkader Zarrouk^a and Youssef Ramli^{b*}

Received 14 November 2024

Accepted 6 December 2024

Edited by L. Van Meervelt, Katholieke Universiteit Leuven, Belgium

Keywords: crystal structure; acetamide; piperidine; hydrogen bond; C=O... π (ring) interaction.

CCDC reference: 2408229

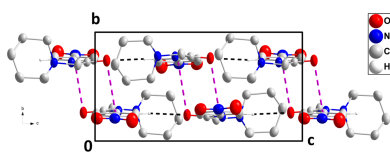
Supporting information: this article has supporting information at journals.iucr.org/e

^aLaboratory of Materials Nanotechnology and Environment, Faculty of Sciences, Mohammed V University in Rabat, PO Box 1014, Rabat, Morocco, ^bLaboratory of Medicinal Chemistry, Drug Sciences Research Center, Faculty of Medicine and Pharmacy, Mohammed V University, Rabat, Morocco, ^cSchool of Chemistry, Cardiff University, Main Building, Park Place, Cardiff, CF10 3AT, United Kingdom, ^dLaboratory of Medicinal Chemistry, Faculty of Clinical Pharmacy, 21 September University, Yemen, and ^eDepartment of Chemistry, Tulane University, New Orleans, LA 70118, USA.
*Correspondence e-mail: alsubaripharmaco@21umas.edu.ye, yramli76@yahoo.fr

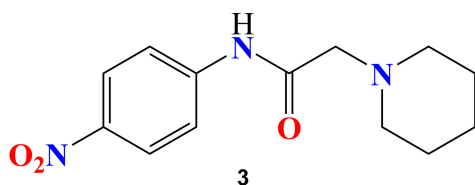
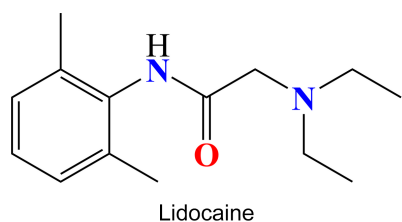
In the title molecule, C₁₃H₁₇N₃O₃, the substituents on the phenyl ring are rotated slightly out of the mean plane of the ring but the piperidine moiety is nearly perpendicular to that plane. In the crystal, C—H...O hydrogen bonds form chains of molecules extending along the *c*-axis direction, which are linked by C=O... π (ring) interactions. A Hirshfeld surface analysis showed the majority of intermolecular interactions to be H...H contacts while O...H/H...O contacts are the second most numerous.

1. Chemical context

Heterocyclic compounds, especially those containing a nitrogen atom, are of substantial interest in medicinal chemistry (El Moutaouakil Ala Allah *et al.*, 2024). Extensive studies of the acetamide family have demonstrated that it can be present in various known drugs of different classes with different therapeutic activities (Rahim *et al.*, 2015; Bennani *et al.*, 2020; Karrouchi *et al.*, 2018). Their structural similarity to various bioactive natural and synthetic molecules grants them a broad spectrum of biological activities (Ettahiri *et al.*, 2024). Lidocaine is a heterocyclic compound that acts as a local anesthetic (Calatayud & Gonzalez, 2003). It consists of a lipophilic aromatic ring and a hydrophilic amine. Its main target in excitable cells is the voltage-gated sodium channel, responsible for the increased sodium permeability observed during the rising phase of the action potential in peripheral nerves, skeletal muscles, as well as in neuroendocrine and cardiac cells (Costa *et al.*, 2008). Continuing our research in this area (Missioui *et al.*, 2022b; Guerrab *et al.*, 2021; Mortada *et al.*, 2024) we synthesized the lidocaine analogue *N*-(4-nitrophenyl)-2-(piperidin-1-yl)acetamide through an alkylation reaction of 2-chloro-*N*-(4-nitrophenyl)acetamide and piperidine, conducted under reflux in toluene. This paper presents the crystal structure of this lidocaine analogue, **3**. A Hirshfeld surface analysis was performed to analyze the intermolecular interactions.



Published under a CC BY 4.0 licence



2. Structural commentary

The title compound, **3**, crystallizes in the monoclinic space group $P2_1/c$ with one molecule in the asymmetric unit (Fig. 1). The nitro group is rotated $2.84(3)^\circ$ out of the mean plane of the attached phenyl ring while the dihedral angle between the plane defined by C8, N2, C7 and O1 and the mean plane of the phenyl ring is $4.52(3)^\circ$. The C1—N1—C6—C7 torsion angle is $92.8(2)^\circ$, which places the mean plane of the piperidine ring nearly perpendicular to the remainder of the molecule, which is particularly evident in Figs. 2 and 4 and is partly due to the intramolecular N2—H2···N1 hydrogen bond (Fig. 1 and Table 1). The piperidine ring adopts a chair conformation with puckering parameters (Cremer & Pople, 1975) $Q = 0.559(2) \text{ \AA}$, $\theta = 178.1(2)^\circ$ and $\varphi = 199(8)^\circ$.

3. Supramolecular features

In the crystal, C13—H13···O1ⁱ hydrogen bonds (Table 1) form chains of molecules extending along the c -axis direction (Fig. 2). These are linked in pairs across centers of symmetry by C7=O1···Cg2 interactions [Cg2 is the centroid of the C8—

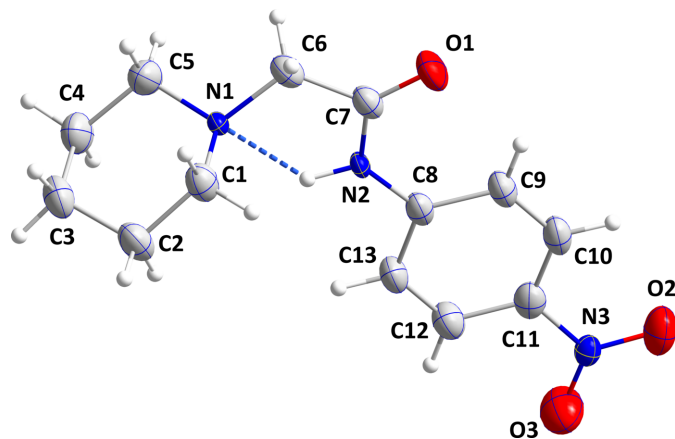


Figure 1
Perspective view of the title molecule with labeling scheme and 30% probability ellipsoids. The intramolecular hydrogen bond is depicted by a dashed line.

Table 1
Hydrogen-bond geometry (\AA , $^\circ$).

$D-H\cdots A$	$D-H$	$H\cdots A$	$D\cdots A$	$D-H\cdots A$
N2—H2···N1	0.91 (1)	2.12 (2)	2.653 (2)	117 (2)
C13—H13···O1 ⁱ	0.93	2.36	3.265 (2)	164

Symmetry code: (i) $x, -y + \frac{3}{2}, z - \frac{1}{2}$.

C13 ring at $-x + 1, -y + 2, -z + 1$; O1···Cg2 = $3.9066(7) \text{ \AA}$, C7···Cg2 = $4.274(2)$, C7=O1···Cg2 = $99.16(12)^\circ$] (Figs. 3 and 4).

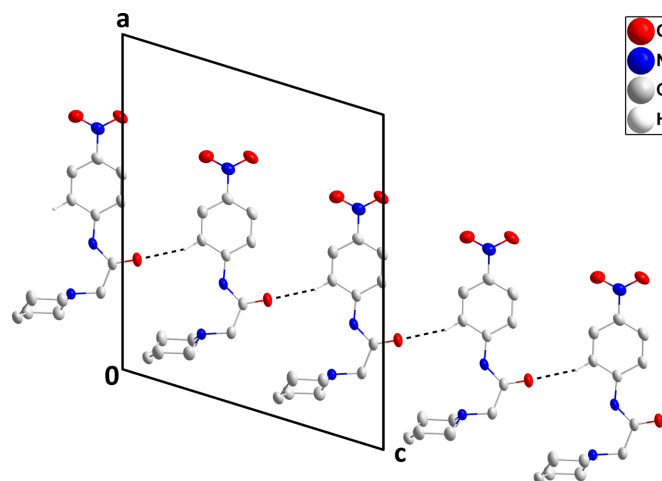


Figure 2
A portion of one chain viewed along the b -axis direction with the intermolecular C—H···O hydrogen bonds depicted by black dashed lines. Hydrogen atoms not involved in these interactions are omitted for clarity.

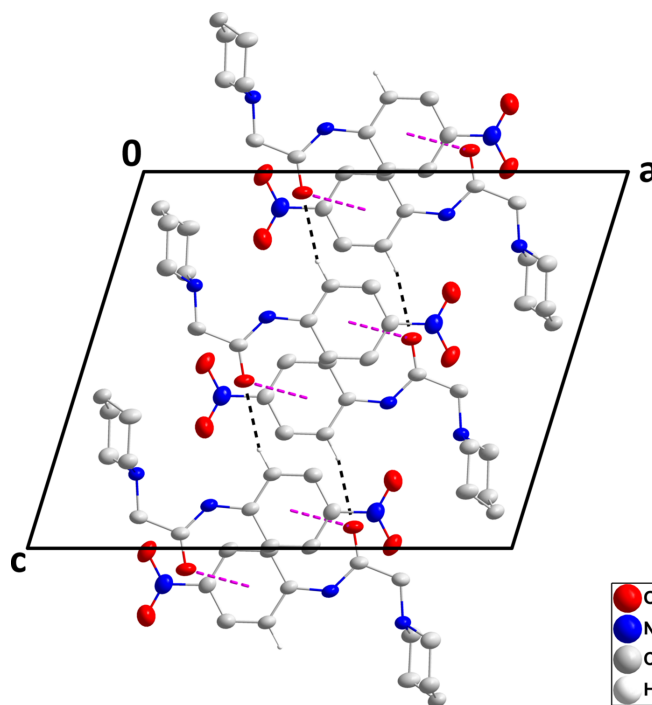


Figure 3
Packing viewed along the b -axis direction showing the pairing of two chains through C=O··· π (ring) interactions (pink dashed lines). The C—H···O hydrogen bonds are depicted by black dashed lines. Hydrogen atoms not involved in these interactions are omitted for clarity.

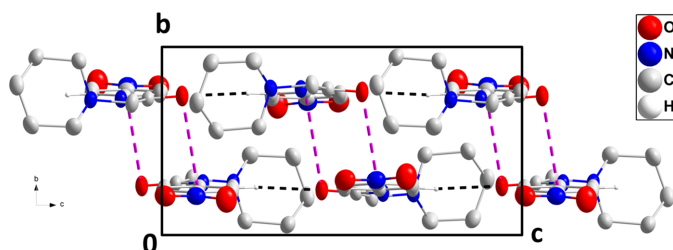


Figure 4
Packing viewed along the *a*-axis direction showing the pairing of two chains through C=O \cdots π (ring) interactions (pink dashed lines). The C–H \cdots O hydrogen bonds are depicted by black dashed lines. Hydrogen atoms not involved in these interactions are omitted for clarity.

4. Database survey

A search of the Cambridge Structural Database (CSD, updated to June 2024 (Groom *et al.*, 2016)) with the search fragment **A** shown in Fig. 5 yielded eleven hits of which five had the fragment as part of multidentate ligands in metal complexes while three more were ionic compounds. None of these were considered relevant for comparison with the title molecule. The three structures that are relevant are shown in Fig. 5.

In MACPAJ (Kang *et al.*, 2010), the rotation of the nitro group out of the plane of the attached phenyl ring is virtually the same as in the title molecule, but the dihedral angle between the mean plane of the acetamido group and that of the phenyl ring is significantly greater at 13.80 (8) $^\circ$. On the other hand, the entire molecule is relatively flat as the mean planes of the phenyl and quinoline moieties are inclined to one another by 8.02 (7) $^\circ$. The packing involves chains of alternating molecules and water molecules, which are formed by N–H \cdots O and O–H \cdots O plus O–H \cdots N hydrogen bonds and are linked by π -stacking interactions between the phenyl and quinoline units.

In QAGNOF (Missioui *et al.*, 2020), the mean planes of the nitro and acetamide groups are inclined to that of the phenyl ring by 5.9 (5) and 14.8 (1) $^\circ$, respectively. The 3-D structure of the crystal consists of corrugated layers parallel to (10 $\bar{2}$), which are formed by C–H \cdots O and C–H \cdots N hydrogen bonds.

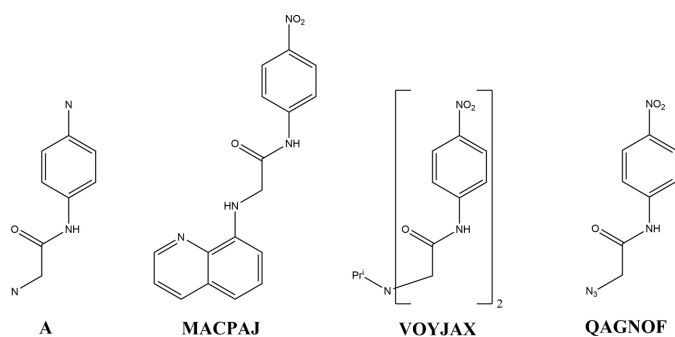


Figure 5
The search fragment used for the Database Survey (**A**) and three relevant hits generated.

There is an intramolecular N–H \cdots O hydrogen bond in VOYJAX (Juraj *et al.*, 2019), which gives the molecule a U-shaped conformation. The dihedral angles between the mean planes of the acetamido groups and their attached phenyl rings are both about 13 $^\circ$, while the nitro group on the portion containing the NH group that forms the intramolecular hydrogen bond is rotated by 8.7 $^\circ$ relative to the plane of its phenyl group, and the other nitro group is rotated by 5.6 $^\circ$. The other NH group forms intermolecular N–H \cdots O hydrogen bonds, generating chains extending along the normal to (201). These are connected into a 3-D network by a large number of C–H \cdots O hydrogen bonds and offset π -stacking interactions.

5. Hirshfeld surface analysis

The Hirshfeld surface analysis was carried out with *Crystal-Explorer* (Spackman *et al.*, 2021) and the descriptions and interpretations of the plots generated have been described previously (Tan *et al.*, 2019). The d_{norm} surface calculated over the range -0.2975 to 1.2755 in arbitrary units is shown in Fig. 6*a* and includes two neighboring molecules attached *via* C–H \cdots O hydrogen bonds, which are also indicated by the dark-red spots. This view corresponds to that in Fig. 2. The Hirshfeld surface calculated over the shape-index function is shown in Fig. 6*b* with the set of blue and orange triangles offset from the center of the benzene ring indicating the C=O \cdots Cg interactions. Fig. 6*c* shows the d_{norm} surface

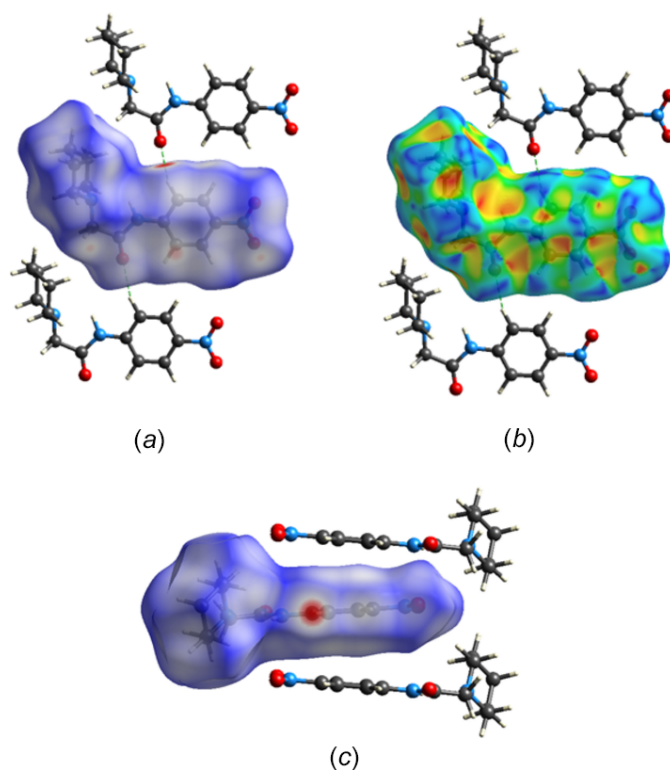


Figure 6
Hirshfeld surfaces: (*a*) d_{norm} viewed perpendicular to the plane of the phenyl ring with two adjacent hydrogen-bonded molecules, (*b*) same view of the shape-index surface, (*c*) d_{norm} viewed parallel to the plane of the phenyl ring with two adjacent stacking molecules.

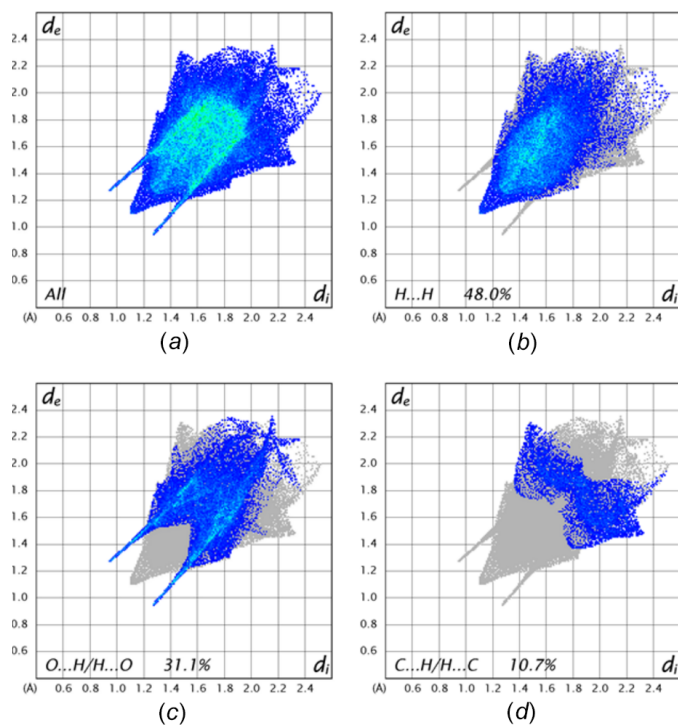


Figure 7
2-D fingerprint plots: (a) all intermolecular interactions, and those delineated into (b) H...H, (c) O...H/H...O and (d) C...H/H...C interactions.

viewed parallel to the plane of the benzene ring and includes two of the adjacent molecules involved in the C=O...C_g stacking interactions. A representation of all intermolecular interactions is given in Fig. 7a with delineations into H...H, O...H/H...O and C...H/H...C interactions, together with their percentage contributions, shown in Fig. 7b–7d, respectively. The high percentage attributed to H...H interactions is a consequence of the high hydrogen content of the molecule and comes significantly from van der Waals contacts involving the piperidine moiety. Second and third in importance are the O...H/H...O and the C...H/H...C contacts with the former appearing as a pair of sharp spikes indicating a narrow range of H...O distances. Despite the presence of C=O...C_g interactions, the O...C/C...O contacts contribute only 2.9% to the total.

6. Synthesis and crystallization

The reaction sequence for title compound **3** is shown in Fig. 8.

Compound **1**, namely 2-chloro-*N*-(4-nitrophenyl)acetamide was synthesized according to the procedure described in the literature (Missioui *et al.*, 2022a; Li *et al.*, 2006). Next,

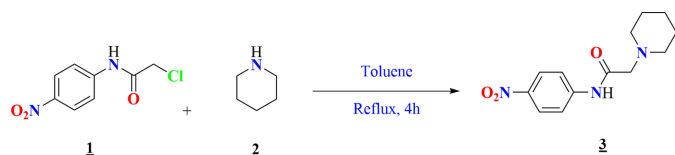


Figure 8
Reaction scheme for the formation of the title compound **3**.

Table 2
Experimental details.

Crystal data	
Chemical formula	C ₁₃ H ₁₇ N ₃ O ₃
<i>M_r</i>	263.29
Crystal system, space group	Monoclinic, <i>P</i> ₂ ₁ / <i>c</i>
Temperature (K)	293
<i>a</i> , <i>b</i> , <i>c</i> (Å)	16.2304 (9), 6.5804 (3), 13.2222 (7)
β (°)	107.156 (6)
<i>V</i> (Å ³)	1349.33 (13)
<i>Z</i>	4
Radiation type	Mo Kα
μ (mm ⁻¹)	0.09
Crystal size (mm)	0.53 × 0.16 × 0.16
Data collection	
Diffractometer	SuperNova, Dual, Cu at home/ near, Atlas
Absorption correction	Gaussian (CrysAlisPr; Rigaku OD, 2023)
<i>T_{min}</i> , <i>T_{max}</i>	0.564, 1.000
No. of measured, independent and observed [<i>I</i> > 2σ(<i>I</i>)] reflections	11819, 3351, 2275
<i>R_{int}</i>	0.030
(sin θ/λ) _{max} (Å ⁻¹)	0.696
Refinement	
R[<i>F</i> ² > 2σ(<i>F</i> ²)], <i>wR</i> (<i>F</i> ²), <i>S</i>	0.059, 0.180, 1.06
No. of reflections	3351
No. of parameters	175
No. of restraints	1
H-atom treatment	H atoms treated by a mixture of independent and constrained refinement
Δρ _{max} , Δρ _{min} (e Å ⁻³)	0.14, -0.21

Computer programs: *CrysAlis PRO* (Rigaku OD, 2023), *SHELXT* (Sheldrick, 2015a), *SHELXL* (Sheldrick, 2015b), *DIAMOND* (Brandenburg & Putz, 2012) and *SHELXTL* (Sheldrick, 2008).

1.2 mmol of piperidine **2** was mixed with **1** mmol of 2-chloro-*N*-(4-nitrophenyl)acetamide in toluene, and the mixture was refluxed for 4 h. Upon completion of the reaction, toluene was removed by liquid–liquid extraction, and the aqueous phase was subsequently acidified with hydrochloric acid, prompting the precipitation of the title compound **3**. The precipitate was filtered, dried, and recrystallized from ethanol, yielding white crystals of the target compound.

Yield = 40%, color: white, m.p. = 401–403 K. FT-IR (ATR, ν, cm⁻¹): 3214 (N–H amide), 2937 (C–H Aliphatic), 1692 (C=O). ¹H NMR (500 MHz, DMSO-*d*₆) δ ppm: 1.34 (*m*, 2H, C–CH₂–C), 1.52 (*quint*, 4H, *J* = 5 Hz, C–CH₂–C), 2.40 (*t*, 4H, *J* = 5 Hz, N–CH₂–), 3.02 (*s*, 2H, CH₂ amide), 7.05–7.65 (*m*, 4H, H–Ar), 9.67 (*s*, 1H, NH_{amide}). ¹³C NMR (125 MHz, DMSO-*d*₆) δ ppm: 25.10 (C–CH₂–C), 24.01 (C–CH₂–C), 53.85 (N–CH₂–C), 61.48 (N–CH₂–C=O), 128.80, 128.21, 135.50, 135.52 (C–Ar), 168.82 (C=O). HRMS (ESI): calculated for C₁₃H₁₇N₃O₃ [*M* + H]⁺ 263.1270; found 264.13318.

7. Refinement

Crystal data, data collection and structure refinement details are summarized in Table 2. Hydrogen atoms attached to carbon were included as riding contributions in idealized positions with isotropic displacement parameters tied to those of the attached atoms. That attached to nitrogen N2 was

located in a difference map and refined with a DFIX 0.91 0.01 instruction.

Acknowledgements

YR is thankful to the National Center for Scientific and Technical Research of Morocco (CNRST) for its continuous support. The contributions of the authors are as follows: conceptualization, YR; methodology, AA; investigation, IM and IN; writing (original draft), JTM and AEMAA; writing (review and editing of the manuscript), YR; formal analysis, YR and JTM; supervision, YR and AZ; crystal structure determination, BMK.

References

- Bennani, F. E., Doudach, L., Cherrah, Y., Ramli, Y., Karrassi, K., Ansar, M. & Faouzi, M. E. A. (2020). *Bioorg. Chem.* **97**, 103470.
- Brandenburg, K. & Putz, H. (2012). *DIAMOND*, Crystal Impact GbR, Bonn, Germany.
- Calatayud, J. & Gonzalez, A. (2003). *Anesthesiology* **98**, 1503–8.
- Costa, J. C. S., Neves, J. S., de Souza, M. V. N., Siqueira, R. A., Romeiro, N. C., Boechat, N., Silva, P. M. R. & Martins, M. A. (2008). *Bioorg. Med. Chem. Lett.* **18**, 1162–1166.
- Cremer, D. & Pople, J. A. (1975). *J. Am. Chem. Soc.* **97**, 1354–1358.
- El Moutaouakil Ala Allah, A., Said, M. A., Al-Kaff, N. S., Mague, J. T., Demirtaş, G. & Ramli, Y. (2024). *J. Mol. Struct.* **1318**, 139430.
- Ettahiri, W., Adardour, M., Alaoui, S., Allah, A. E. A., Aichouch, M., Salim, R., Ramli, Y., Bouyahya, A. & Taleb, M. (2024). *Phytochem. Lett.* **61**, 247–269.
- Groom, C. R., Bruno, I. J., Lightfoot, M. P. & Ward, S. C. (2016). *Acta Cryst.* **B72**, 171–179.
- Guerrab, W., Missioui, M., Zaoui, Y., Mague, J. T. & Ramli, Y. (2021). *Z. Kristallogr. New Cryst. Struct.* **236**, 133–134.
- Kang, J., Jang, S. P., Kim, Y.-H., Lee, J. H., Park, E. B., Lee, H. G., Kim, J. H., Kim, Y., Kim, S.-J. & Kim, C. (2010). *Tetrahedron Lett.* **51**, 6658–6662.
- Karrassi, K., Radi, S., Ramli, Y., Taoufik, J., Mabkhot, Y. N., Al-aizari, F. A. & Ansar, M. (2018). *Molecules*, **23**, 134–220.
- Missioui, M., Guerrab, W., Mague, J. T. & Ramli, Y. (2020). *Z. Kristallogr. New Cryst. Struct.* **235**, 1429–1430.
- Missioui, M., Guerrab, W., Nchioua, I., El Moutaouakil Ala Allah, A., Kalonji Mubengayi, C., Alsubari, A., Mague, J. T. & Ramli, Y. (2022a). *Acta Cryst.* **E78**, 687–690.
- Missioui, M., Lgaz, H., Guerrab, W., Lee, H., Warad, I., Mague, J. T., Ali, I. H., Essassi, E. M. & Ramli, Y. (2022b). *J. Mol. Struct.* **1253**, 132132.
- Mortada, S., Guerrab, W., Missioui, M., Salhi, N., Naceiri Mrabti, H., Rouass, L., Benkirane, S., Hassane, M., Masrar, A., Mezzour, H., Faouzi, M. E. A. & Ramli, Y. (2024). *J. Biomol. Struct. Dyn.* **42**, 6711–6725.
- Pantalon Juraj, N., Miletić, G. I., Perić, B., Popović, Z., Smrečki, N., Vianello, R. & Kirin, S. I. (2019). *Inorg. Chem.* **58**, 16445–16457.
- Rahim, F., Ullah, H., Javid, M. T., Wadood, A., Taha, M., Ashraf, M., Shaukat, A., Junaid, M., Hussain, S., Rehman, W., Mehmood, R., Sajid, M., Khan, M. N. & Khan, K. M. (2015). *Bioorg. Chem.* **62**, 15–21.
- Rigaku OD (2023). *CrysAlis PRO*. Rigaku Oxford Diffraction, Yarnton, England.
- Sheldrick, G. M. (2008). *Acta Cryst.* **A64**, 112–122.
- Sheldrick, G. M. (2015a). *Acta Cryst.* **A71**, 3–8.
- Sheldrick, G. M. (2015b). *Acta Cryst.* **C71**, 3–8.
- Spackman, P. R., Turner, M. J., McKinnon, J. J., Wolff, S. K., Grimwood, D. J., Jayatilaka, D. & Spackman, M. A. (2021). *J. Appl. Cryst.* **54**, 1006–1011.
- Tan, S. L., Jotani, M. M. & Tiekink, E. R. T. (2019). *Acta Cryst.* **E75**, 308–318.
- Wen, Y.-H., Li, X.-M., Xu, L.-L., Tang, X.-F. & Zhang, S.-S. (2006). *Acta Cryst.* **E62**, o4427–o4428.

supporting information

Acta Cryst. (2025). E81, 69-73 [https://doi.org/10.1107/S205698902401185X]

Crystal structure and Hirshfeld surface analysis of *N*-(4-nitrophenyl)-2-(piperidin-1-yl)acetamide (lidocaine analogue)

Imane Maimoune, Benson M. Kariuki, Abderrazzak El Moutaouakil Ala Allah, Intissar Nchioua, Abdulsalam Alsubari, Joel T. Mague, Abdelkader Zarrouk and Youssef Ramli

Computing details

N-(4-Nitrophenyl)-2-(piperidin-1-yl)acetamide

Crystal data

$C_{13}H_{17}N_3O_3$

$M_r = 263.29$

Monoclinic, $P2_1/c$

$a = 16.2304$ (9) Å

$b = 6.5804$ (3) Å

$c = 13.2222$ (7) Å

$\beta = 107.156$ (6)°

$V = 1349.33$ (13) Å³

$Z = 4$

$F(000) = 560$

$D_x = 1.296$ Mg m⁻³

Mo $K\alpha$ radiation, $\lambda = 0.71073$ Å

Cell parameters from 4698 reflections

$\theta = 4.1$ – 28.9 °

$\mu = 0.09$ mm⁻¹

$T = 293$ K

Block, colourless

$0.53 \times 0.16 \times 0.16$ mm

Data collection

SuperNova, Dual, Cu at home/near, Atlas diffractometer

Detector resolution: 10.5082 pixels mm⁻¹

ω scans

Absorption correction: gaussian
(CrysAlisPr; Rigaku OD, 2023)

$T_{\min} = 0.564$, $T_{\max} = 1.000$

11819 measured reflections

3351 independent reflections

2275 reflections with $I > 2\sigma(I)$

$R_{\text{int}} = 0.030$

$\theta_{\max} = 29.7$ °, $\theta_{\min} = 3.4$ °

$h = -22 \rightarrow 17$

$k = -8 \rightarrow 9$

$l = -13 \rightarrow 18$

Refinement

Refinement on F^2

Least-squares matrix: full

$R[F^2 > 2\sigma(F^2)] = 0.059$

$wR(F^2) = 0.180$

$S = 1.06$

3351 reflections

175 parameters

1 restraint

Primary atom site location: dual

Secondary atom site location: difference Fourier map

Hydrogen site location: mixed

H atoms treated by a mixture of independent and constrained refinement

$w = 1/[\sigma^2(F_o^2) + (0.0632P)^2 + 0.563P]$

where $P = (F_o^2 + 2F_c^2)/3$

$(\Delta/\sigma)_{\max} < 0.001$

$\Delta\rho_{\max} = 0.14$ e Å⁻³

$\Delta\rho_{\min} = -0.21$ e Å⁻³

Special details

Geometry. All esds (except the esd in the dihedral angle between two l.s. planes) are estimated using the full covariance matrix. The cell esds are taken into account individually in the estimation of esds in distances, angles and torsion angles; correlations between esds in cell parameters are only used when they are defined by crystal symmetry. An approximate (isotropic) treatment of cell esds is used for estimating esds involving l.s. planes.

Refinement. Refinement of F^2 against ALL reflections. The weighted R-factor wR and goodness of fit S are based on F^2 , conventional R-factors R are based on F , with F set to zero for negative F^2 . The threshold expression of $F^2 > 2\sigma(F^2)$ is used only for calculating R-factors(gt) etc. and is not relevant to the choice of reflections for refinement. R-factors based on F^2 are statistically about twice as large as those based on F , and R-factors based on ALL data will be even larger. H-atoms attached to carbon were placed in calculated positions ($C-H = 0.95 - 0.98 \text{ \AA}$) and were included as riding contributions with isotropic displacement parameters 1.2 - 1.5 times those of the attached atoms. That attached to nitrogen was placed in a location derived from a difference map and refined with a DFIX 0.91 0.01 instruction.

Fractional atomic coordinates and isotropic or equivalent isotropic displacement parameters (\AA^2)

	<i>x</i>	<i>y</i>	<i>z</i>	$U_{\text{iso}}^*/U_{\text{eq}}$
O1	0.34083 (11)	0.7609 (2)	0.55602 (11)	0.0715 (5)
O2	0.75115 (11)	0.7076 (3)	0.49135 (16)	0.0883 (6)
O3	0.71190 (13)	0.6897 (4)	0.32098 (19)	0.1075 (7)
N1	0.17750 (10)	0.7809 (2)	0.30235 (12)	0.0514 (4)
N2	0.34754 (11)	0.7767 (3)	0.38608 (12)	0.0544 (4)
H2	0.3113 (14)	0.794 (4)	0.3199 (11)	0.082*
N3	0.69567 (13)	0.7073 (3)	0.40483 (19)	0.0725 (6)
C1	0.15223 (15)	0.5745 (3)	0.26946 (15)	0.0637 (6)
H1A	0.103397	0.535977	0.293408	0.076*
H1B	0.199494	0.482909	0.301768	0.076*
C2	0.12820 (17)	0.5550 (4)	0.15026 (17)	0.0738 (7)
H2A	0.178609	0.580913	0.127050	0.089*
H2B	0.108885	0.417421	0.129819	0.089*
C3	0.05749 (15)	0.7031 (4)	0.09660 (17)	0.0699 (6)
H3A	0.047410	0.698021	0.020587	0.084*
H3B	0.004423	0.665403	0.111393	0.084*
C4	0.08291 (16)	0.9145 (4)	0.13599 (17)	0.0726 (7)
H4A	0.034863	1.005917	0.106948	0.087*
H4B	0.130725	0.959234	0.111583	0.087*
C5	0.10881 (16)	0.9242 (4)	0.25522 (17)	0.0706 (6)
H5A	0.128024	1.060726	0.278232	0.085*
H5B	0.059199	0.893836	0.279295	0.085*
C6	0.20950 (14)	0.7987 (4)	0.41715 (15)	0.0635 (6)
H6A	0.181932	0.695836	0.448581	0.076*
H6B	0.193088	0.930527	0.437812	0.076*
C7	0.30609 (14)	0.7755 (3)	0.46103 (14)	0.0539 (5)
C8	0.43526 (12)	0.7593 (3)	0.39598 (14)	0.0484 (4)
C9	0.49923 (14)	0.7525 (3)	0.49329 (16)	0.0564 (5)
H9	0.484448	0.759105	0.556019	0.068*
C10	0.58435 (14)	0.7361 (3)	0.49582 (17)	0.0597 (5)
H10	0.627409	0.731472	0.560310	0.072*
C11	0.60535 (13)	0.7267 (3)	0.40304 (17)	0.0561 (5)
C12	0.54306 (15)	0.7333 (3)	0.30645 (17)	0.0648 (6)

H12	0.558375	0.726652	0.244073	0.078*
C13	0.45840 (14)	0.7497 (3)	0.30335 (15)	0.0588 (5)
H13	0.415929	0.754475	0.238376	0.071*

Atomic displacement parameters (Å²)

	U^{11}	U^{22}	U^{33}	U^{12}	U^{13}	U^{23}
O1	0.0773 (10)	0.0929 (12)	0.0357 (7)	−0.0018 (8)	0.0035 (7)	0.0013 (7)
O2	0.0574 (9)	0.0966 (13)	0.0938 (14)	−0.0027 (8)	−0.0041 (9)	0.0062 (10)
O3	0.0747 (12)	0.155 (2)	0.0976 (16)	0.0010 (12)	0.0324 (11)	0.0016 (14)
N1	0.0505 (8)	0.0634 (10)	0.0369 (8)	0.0029 (7)	0.0078 (6)	−0.0033 (7)
N2	0.0536 (9)	0.0673 (10)	0.0343 (8)	0.0003 (8)	0.0008 (7)	0.0000 (7)
N3	0.0610 (11)	0.0701 (12)	0.0798 (14)	−0.0034 (9)	0.0108 (10)	0.0025 (10)
C1	0.0731 (14)	0.0621 (13)	0.0494 (11)	−0.0004 (10)	0.0079 (10)	0.0051 (9)
C2	0.0935 (17)	0.0671 (14)	0.0507 (12)	−0.0034 (12)	0.0053 (11)	−0.0092 (10)
C3	0.0600 (12)	0.0934 (17)	0.0477 (11)	−0.0108 (12)	0.0026 (9)	0.0027 (11)
C4	0.0769 (15)	0.0764 (15)	0.0562 (12)	0.0126 (12)	0.0067 (11)	0.0133 (11)
C5	0.0784 (15)	0.0684 (14)	0.0596 (13)	0.0169 (11)	0.0122 (11)	−0.0009 (11)
C6	0.0672 (13)	0.0820 (15)	0.0397 (10)	0.0038 (11)	0.0132 (9)	−0.0078 (10)
C7	0.0652 (12)	0.0547 (11)	0.0364 (9)	−0.0022 (9)	0.0067 (8)	−0.0030 (8)
C8	0.0550 (11)	0.0428 (9)	0.0391 (9)	−0.0023 (8)	0.0012 (8)	−0.0008 (7)
C9	0.0601 (11)	0.0617 (12)	0.0380 (9)	−0.0029 (9)	−0.0001 (8)	0.0002 (8)
C10	0.0597 (12)	0.0561 (11)	0.0491 (11)	−0.0030 (9)	−0.0058 (9)	0.0015 (9)
C11	0.0557 (11)	0.0460 (10)	0.0590 (12)	−0.0027 (8)	0.0052 (9)	0.0020 (8)
C12	0.0682 (14)	0.0749 (14)	0.0471 (11)	−0.0011 (11)	0.0105 (10)	0.0012 (10)
C13	0.0589 (12)	0.0707 (13)	0.0383 (9)	0.0004 (9)	0.0010 (8)	−0.0001 (9)

Geometric parameters (Å, °)

O1—C7	1.219 (2)	C4—C5	1.508 (3)
O2—N3	1.230 (3)	C4—H4A	0.9700
O3—N3	1.218 (3)	C4—H4B	0.9700
N1—C1	1.448 (3)	C5—H5A	0.9700
N1—C5	1.453 (3)	C5—H5B	0.9700
N1—C6	1.457 (2)	C6—C7	1.510 (3)
N2—C7	1.352 (3)	C6—H6A	0.9700
N2—C8	1.396 (3)	C6—H6B	0.9700
N2—H2	0.906 (10)	C8—C13	1.384 (3)
N3—C11	1.465 (3)	C8—C9	1.395 (2)
C1—C2	1.513 (3)	C9—C10	1.376 (3)
C1—H1A	0.9700	C9—H9	0.9300
C1—H1B	0.9700	C10—C11	1.368 (3)
C2—C3	1.513 (3)	C10—H10	0.9300
C2—H2A	0.9700	C11—C12	1.376 (3)
C2—H2B	0.9700	C12—C13	1.367 (3)
C3—C4	1.500 (3)	C12—H12	0.9300
C3—H3A	0.9700	C13—H13	0.9300
C3—H3B	0.9700		

C1—N1—C5	111.50 (17)	N1—C5—C4	111.27 (18)
C1—N1—C6	111.77 (17)	N1—C5—H5A	109.4
C5—N1—C6	112.78 (16)	C4—C5—H5A	109.4
C7—N2—C8	130.18 (16)	N1—C5—H5B	109.4
C7—N2—H2	112.8 (17)	C4—C5—H5B	109.4
C8—N2—H2	117.0 (17)	H5A—C5—H5B	108.0
O3—N3—O2	123.5 (2)	N1—C6—C7	113.75 (17)
O3—N3—C11	118.5 (2)	N1—C6—H6A	108.8
O2—N3—C11	118.0 (2)	C7—C6—H6A	108.8
N1—C1—C2	110.83 (17)	N1—C6—H6B	108.8
N1—C1—H1A	109.5	C7—C6—H6B	108.8
C2—C1—H1A	109.5	H6A—C6—H6B	107.7
N1—C1—H1B	109.5	O1—C7—N2	125.2 (2)
C2—C1—H1B	109.5	O1—C7—C6	121.1 (2)
H1A—C1—H1B	108.1	N2—C7—C6	113.72 (16)
C3—C2—C1	111.1 (2)	C13—C8—C9	119.5 (2)
C3—C2—H2A	109.4	C13—C8—N2	117.15 (16)
C1—C2—H2A	109.4	C9—C8—N2	123.38 (19)
C3—C2—H2B	109.4	C10—C9—C8	119.6 (2)
C1—C2—H2B	109.4	C10—C9—H9	120.2
H2A—C2—H2B	108.0	C8—C9—H9	120.2
C4—C3—C2	109.97 (18)	C11—C10—C9	119.71 (18)
C4—C3—H3A	109.7	C11—C10—H10	120.1
C2—C3—H3A	109.7	C9—C10—H10	120.1
C4—C3—H3B	109.7	C10—C11—C12	121.4 (2)
C2—C3—H3B	109.7	C10—C11—N3	120.15 (19)
H3A—C3—H3B	108.2	C12—C11—N3	118.4 (2)
C3—C4—C5	111.44 (19)	C13—C12—C11	119.2 (2)
C3—C4—H4A	109.3	C13—C12—H12	120.4
C5—C4—H4A	109.3	C11—C12—H12	120.4
C3—C4—H4B	109.3	C12—C13—C8	120.65 (18)
C5—C4—H4B	109.3	C12—C13—H13	119.7
H4A—C4—H4B	108.0	C8—C13—H13	119.7
C5—N1—C1—C2	58.7 (2)	C7—N2—C8—C9	-5.4 (3)
C6—N1—C1—C2	-174.01 (19)	C13—C8—C9—C10	-0.1 (3)
N1—C1—C2—C3	-56.4 (3)	N2—C8—C9—C10	-179.68 (18)
C1—C2—C3—C4	53.3 (3)	C8—C9—C10—C11	0.0 (3)
C2—C3—C4—C5	-53.0 (3)	C9—C10—C11—C12	0.0 (3)
C1—N1—C5—C4	-58.5 (3)	C9—C10—C11—N3	-179.44 (18)
C6—N1—C5—C4	174.8 (2)	O3—N3—C11—C10	176.6 (2)
C3—C4—C5—N1	55.8 (3)	O2—N3—C11—C10	-2.7 (3)
C1—N1—C6—C7	92.8 (2)	O3—N3—C11—C12	-2.9 (3)
C5—N1—C6—C7	-140.7 (2)	O2—N3—C11—C12	177.9 (2)
C8—N2—C7—O1	1.2 (3)	C10—C11—C12—C13	0.0 (3)
C8—N2—C7—C6	179.99 (19)	N3—C11—C12—C13	179.48 (19)
N1—C6—C7—O1	-170.56 (18)	C11—C12—C13—C8	-0.1 (3)

N1—C6—C7—N2	10.6 (3)	C9—C8—C13—C12	0.2 (3)
C7—N2—C8—C13	175.02 (19)	N2—C8—C13—C12	179.75 (19)

Hydrogen-bond geometry (Å, °)

<i>D</i> —H \cdots <i>A</i>	<i>D</i> —H	H \cdots <i>A</i>	<i>D</i> \cdots <i>A</i>	<i>D</i> —H \cdots <i>A</i>
N2—H2 \cdots N1	0.91 (1)	2.12 (2)	2.653 (2)	117 (2)
C13—H13 \cdots O1 ⁱ	0.93	2.36	3.265 (2)	164

Symmetry code: (i) $x, -y+3/2, z-1/2$.